Role of ionization–excitation processes in the cross section for direct ionization of heavy atomic ions by electron impact

Article *in* Physical Review A · October 2014

Impact Factor: 2.81 · DOI: 10.1103/PhysRevA.90.044701

4 authors, including:

J.L. Zeng
National University of Defense Technology

Jianmin Yuan
National University of Defense Technology

Role of ionization-excitation processes in the cross section for direct ionization of heavy atomic ions by electron impact

J. L. Zeng,[*] L. P. Liu, P. F. Liu, and J. M. Yuan

College of Science, National University of Defense Technology, Changsha Hunan, People's Republic of China, 410073

(Received 22 August 2014; published 23 October 2014)

The contribution to the ionization cross section of ionization-excitation processes by electron impact is usually negligibly small for low- and medium-Z elements. We demonstrate here, however, that for heavy atomic ions with the outermost shell being nd ($n = 4,5$) the ionization-excitation processes play an evident role in the ionization cross section. For the $4s^2 4p^6 4d^{10}$ ground level of Gd^{18+}, the ionization-excitation cross section due to the excitation of levels in the $4s^2 4p^6 4d^8 4f$ configuration is comparable to the direct $4p$ and $4s$ ionization cross sections of $(4s^2 4p^5 4d^{10})_{1/2}$ and $(4s 4p^6 4d^{10})_{1/2}$. The total ionization cross section will be underestimated by 15% without including the contribution from ionization-excitation processes. This is a general conclusion for heavy atomic ions, which is verified by taking Pd-like ions of Sn^{4+}, Ba^{10+}, Nd^{14+}, Tb^{19+}, Yb^{24+}, and W^{28+} as examples. The role of ionization-excitation processes can be understood from the overlapping of the wave functions between the $4d$ and $4f$ orbitals.

DOI: 10.1103/PhysRevA.90.044701 PACS number(s): 34.80.Dp, 32.80.Hd

I. INTRODUCTION

Apart from its fundamental importance, the electron impact ionization (EII) cross section has practical applications in plasma modeling in both astrophysical and laboratory plasmas [1–3]. Most EII researches have focused on the light- and medium-Z elements, as reviewed by Mattioli *et al.* [4] and Dere [5] for elements from hydrogen to germanium. In contrast, relatively fewer publications have reported the EII cross section of heavy elements. There is intrinsic difficulty in accurate determination of the EII cross section of heavy atoms and atomic ions, both experimentally and theoretically. Experimentally, it is challenging work to produce well-characterized ground-state ion beams. The contributions from metastable ions are inevitably found in experiment [6,7]. Theoretically, for heavy ionic system, the complex electronic structure makes it challenging to accurately determine the cross section. Electron impact in channels of autoionized states can give rise to complicated sequential and direct double or even multiple autoionizations [8–11]. It is a troublesome task to track the Auger and radiative decay pathways.

There is an increasing need to accurately determine the EII cross section and rate coefficients of heavy ions in a variety of research fields such as ultraviolet radiation (EUV) lithography, and magnetic confinement fusion. EUV lithography at 13.5 nm represents the next significant step in the reduction of feature sizes on integrated circuits [12]. Tin ($Z = 50$) and xenon ($Z = 54$) are strong emitters around 13.5 nm, and hence the physical properties such as the radiative opacity [13] and EII cross section are important in understanding the physics of EUV light generation and transport. Very recently, Borovik *et al.* [6] and Pindzola *et al.* [7] experimentally measured the EII cross sections of tin and xenon ions from the threshold up to 1000 eV. Now researchers are considering further reducing the wavelength to around 6.5 nm, which is produced by even heavier elements such as gadolinium ($Z = 64$) and terbium ($Z = 65$) [14–17]. In the area of magnetic confinement fusion reactors, tungsten ($Z = 74$) is receiving considerable attention as a plasma-facing material. The EII cross section is required, yet available data are scarce [18,19]. Recently, Moy *et al.* [20] experimentally investigated the M-shell EII cross section of U ($Z = 92$). For light- and medium-Z elements, many studies were carried out using close-coupling and distorted-wave methods [4,5,21–30]. However, theoretical results are noticeably lacking for the EII cross section of heavy ions.

There are direct and indirect ionization channels for EII processes. As the atomic number increases, the contribution from the indirect processes becomes more and more important. Mattioli *et al.* [4] pointed out that previously proposed EII cross sections are often underestimated due to the neglect of indirect processes for medium-Z elements. For heavy ions, such an underestimation becomes even more pronounced, as demonstrated here.

In this work, we investigate the role of ionization-excitation processes in the cross section for direct ionization of heavy atomic ions by electron impact, taking Pd-like ions as examples. Ionization with simultaneous excitation is significantly more correlated, and hence its contribution to the ionization cross section is usually small compared with that of direct ionization processes [31,32]. Our results show, however, that the ionization cross section can be underestimated by about 15% if one neglect the contributions of ionization-excitation processes for heavy ions.

II. THEORETICAL METHOD

The calculation of the level-to-level ionization cross section was carried out using a fine-structure level distorted wave approximation implemented by the Flexible Atomic Code (FAC) developed by Gu [33]. The direct ionization cross section from an initial state ψ_i to a final state ψ_f can be expressed as

$$\frac{d\sigma_{\rm if}(\varepsilon_0,\varepsilon)}{d\varepsilon} = \frac{2\pi}{k_i^2 g_i} \sum_{\kappa_i\kappa_{f1}\kappa_{f2}} \sum_{J_T} (2J_T+1) \left| \langle \psi_i\kappa_i, J_T M_T | \times \sum_{p<q} \frac{1}{r_{pq}} |\psi_f \kappa_{f1}\kappa_{f2}, J_T M_T\rangle \right|^2, \quad (1)$$

[*] jlzeng@nudt.edu.cn

where ε_0 and k_i are the energy and kinetic momentum of the incident electron; ε is the energy of the ejected electron; g_i is the statistical weight of the initial state; κ_i, κ_{f1}, and κ_{f2} are the relativistic angular quantum numbers of the incident, scattered, and ejected electrons; J_T is the total angular momentum when the target state is coupled to the continuum orbital; and M_T is the projection of the total angular momentum. The energy reservation holds for the process, i.e., $\varepsilon_0 = I + \varepsilon_1 + \varepsilon$, where ε_1 is the energy of scattered electron and I is the ionization potential from the initial state ψ_i to the final state ψ_f. The wave function ψ_i is represented by a linear combination of configuration state functions (CSFs), which are antisymmetric sums of the products of N one-electron Dirac spinors [8,33]. The wave function ψ_f is similarly obtained with one less bound electron. To solve the Dirac spinors of ψ_i and ψ_f, local central potentials, which include the contribution from the nuclear charge and electron-electron interaction of the N and $N-1$ electron systems, are used. The detailed expression of the local central potential of the respective ion can be found in Gu [33]. The wave functions of the continuum orbitals are obtained by solving the Dirac equations with the same central potential as the bound orbitals. The ionization cross section from ψ_i to ψ_f is obtained from

$$\sigma_{\mathrm{if}}(\varepsilon_0) = \int_0^{\frac{\varepsilon_0 - I}{2}} \frac{d\sigma(\varepsilon_0,\varepsilon)}{d\varepsilon} d\varepsilon. \tag{2}$$

The energy conservation relation means that the total energy of the scattered and ejected electrons is fixed but the energy of any one electron can be varied from zero to the maximum, $\varepsilon_0 - I$. Thus we set an upper limit $(\varepsilon_0 - I)/2$ in the integration to avoid a double counting of the continuum states.

Specifically, we investigate the ionization cross section of heavy ions from the threshold to 4000 eV, taking Pd-like ions as examples. The ground configuration of Pd-like ions is $[\mathrm{Ni}]4s^2 4p^6 4d^{10}$. Here [Ni] means a Ni-like electron structure; that is, the orbitals of $1s$, $2s$, $2p$, $3s$, $3p$, and $3d$ are fully occupied. The direct ionization of electrons from these orbitals will result in higher ionization stages rather than single ionization. The direct ionization processes of Pd-like ions are shown schematically as

$$e + 4s^2 4p^6 4d^{10} \rightarrow \begin{cases} 4s^2 4p^6 4d^9 + 2e, \\ 4s^2 4p^5 4d^{10} + 2e, \\ 4s 4p^6 4d^{10} + 2e. \end{cases} \tag{3}$$

They include the direct ionization of $4d$, $4p$, and $4s$ electrons. However, they do not include contributions from ionization-excitation processes. To include them, we should further consider the following processes:

$$e + 4s^2 4p^6 4d^{10} \rightarrow \begin{cases} 4s^2 4p^6 4d^8 nl + 2e, \\ 4s^2 4p^5 4d^9 nl + 2e, \\ 4s 4p^6 4d^9 nl + 2e. \end{cases} \tag{4}$$

These processes refer to direct ionization of $4d$, $4p$, and $4s$ electrons with simultaneous excitation of a $4d$ electron to a higher orbital nl. In principle, simultaneous excitation of a $4p$ or $4s$ electron is also possible, but the cross section from these processes is very small, and thus we do not consider them here. The total ionization cross section is a summation of processes included in Eqs. (3) and (4).

III. RESULTS AND DISCUSSION

We first investigate the detailed level-to-level ionization cross section for Pd-like Gd^{18+}. The first ionization potentials (IPs) of Gd^{18+} and Gd^{19+} are calculated to be 559.1 and 595.4 eV, respectively. To the best of our knowledge, there are no experimental data for IPs of Gd^{18+} and Gd^{19+} ions [34]. Rodrigues *et al.* [35] calculated these values to be 565.0 and 601.0 eV in the Dirac-Fock approximation, which is about 6 eV higher than our results. The difference is because the electron correlations were neglected in the calculations of Rodrigues *et al.* [35]. To verify it, we also calculated these data using the Dirac-Fock approximation, and the results are 564.2 and 600.0 eV, which are in good agreement with those of Rodrigues *et al.* [35]. According to our calculation, the ionization thresholds are 559.1, 687.1, and 802.5 eV for direct ionization of the $4d$, $4p$, and $4s$ subshell electrons of Gd^{18+}, respectively. Ionization of $3d$, $3p$, and $3s$ electrons will result in double ionization. The thresholds of direct ionization and ionization-excitation processes relevant to our discussion are given in Table I. There are too many ionization-excitation channels, and only a few that have relatively larger cross sections are given. By inspecting Table I, we know that the direct ionization of the $4d$, $4p$, and $4s$ electrons of Gd^{18+} produces Gd^{19+} since the IP of these orbitals is less than the summation of the IPs of Gd^{18+} and Gd^{19+}. Also the ionization excitation to configurations of $4s^2 4p^6 4d^8 4f$ and $4s^2 4p^5 4d^9 4f$ produces Gd^{19+}. These two configurations are the most dominant channels of ionization-excitation processes.

Figure 1 shows the direct ionization and ionization-excitation cross section (in units of 1 Mb $= 10^{-18}$ cm^2) from the $4s^2 4p^6 4d^{10}$ ground level of Gd^{18+} to the levels given in Table I. The cross sections corresponding to 1–2, 1–3, 1–4, 1–8, and 1–10 represent the direct ionization of $4d$, $4p$, and $4s$ electrons, while the others denote the ionization-excitation cross sections. Obviously, the direct ionization cross section

TABLE I. Calculated ionization potentials (IP) for direct ionization and for a few ionization-excitation channels of the $4s^2 4p^6 4d^{10}$ ground level of Gd^{18+}.

No.	Level	IP(eV)
1	$(4s^2 4p^6 4d^{10})_0$	0.0
2	$(4s^2 4p^6 4d^9)_{5/2}$	559.09
3	$(4s^2 4p^6 4d^9)_{3/2}$	565.89
4	$(4s^2 4p^5 4d^{10})_{3/2}$	687.11
5	$4s^2 4p^6 4d_{3/2}^4[(4d_{5/2}^4)_2 4f_{5/2}]_{1/2}$	707.55
6	$4s^2 4p^6 4d_{5/2}^6[(4d_{3/2}^2)_2 4f_{5/2}]_{1/2}$	718.45
7	$4s^2 4p^6[(4d_{3/2}^3 4d_{5/2}^5)_2 4f_{5/2}]_{1/2}$	721.32
8	$(4s^2 4p^5 4d^{10})_{1/2}$	748.48
9	$4s^2 4p^6[(4d_{3/2}^3 4d_{5/2}^5)_4 4f_{7/2}]_{1/2}$	761.04
10	$(4s 4p^6 4d^{10})_{1/2}$	802.48
11	$4s^2[4p_{1/2}^2(4p_{3/2}^3 4d_{3/2}^3)_3 4d_{5/2}^6 4f_{5/2}]_{1/2}$	898.12

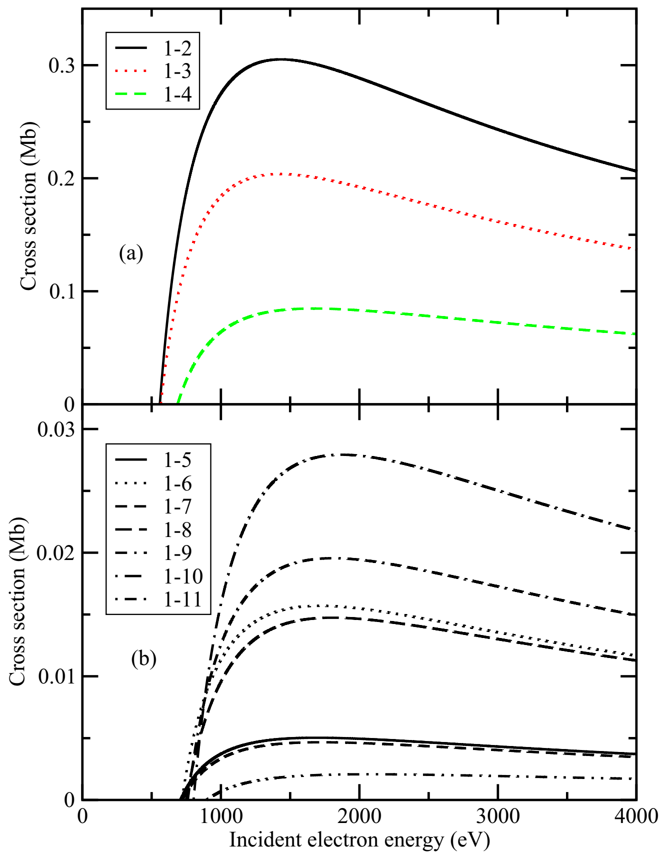

FIG. 1. (Color online) Level-to-level direct ionization and ionization-excitation cross section (1 Mb = 10^{-18} cm^2) of the $4s^24p^64d^{10}$ ground level of Gd^{18+}. The numbers for each line are defined in Table I. The lines corresponding to 1–5, 1–6, 1–7, 1–9, and 1–11 represent the ionization-excitation cross section.

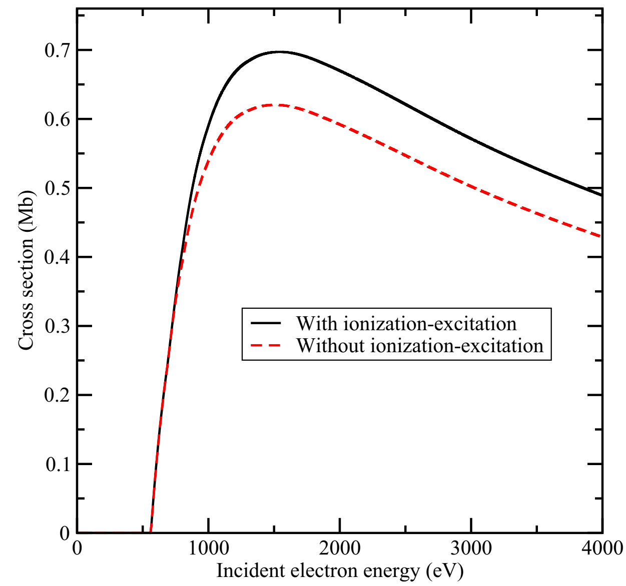

FIG. 2. (Color online) Ionization cross section of the ground level of Gd^{18+} with and without contributions from the ionization-excitation processes.

of the $4d$ electron (1–2 and 1–3 in Fig. 1) is much larger than that of $4p$ and $4s$ ionization. Surprisingly, the ionization-excitation cross sections of 1–5, 1–6, 1–7, 1–9, and 1–11 are comparable to the direct ionization cross sections of $4p$ and $4s$ electrons. We say this is surprising because we know that the ionization-excitation processes are more correlated than the simple direct single-ionization processes. Therefore the cross section from ionization-excitation processes is usually much smaller than that from direct single ionization. Here we see that some channels of ionization excitation have cross sections comparable to those of direct ionization. Such a conclusion shows that the ionization-excitation cross section cannot be neglected in the calculation of the single-ionization cross section. The physical effects due to ionization-excitation processes can more clearly be seen in Fig. 2, which shows the ionization cross section of the ground level of Gd^{18+} with and without the contributions of ionization-excitation processes (solid and dashed lines, respectively). In the incident electron energy range from the ionization threshold (559.1 eV) to about 700 eV, the ionization-excitation channels are closed and hence do not contribute to the ionization cross section. Above the incident electron energy of 1000 eV, the ionization cross section is evidently enhanced by the ionization-excitation processes. Without the contribution of the ionization-excitation processes, the ionization cross section is underestimated by 9.5% at the incident electron energy of 1000 eV. Such an underestimation is increased to 12.5% at 1500 eV and then basically reaches a consistent value of about 15%. The dominant channels of the ionization-excitation processes originate from levels of the $4s^24p^64d^84f$ and $4s^24p^54d^94f$ configurations. The contribution from the $4s^24p^64d^84f$ configuration is, in general larger, than that of $4s^24p^54d^94f$.

For heavy ions, a general phenomenon is that the ionization-excitation processes make a relatively large contribution to the cross section for direct ionization of heavy atomic ions by electron impact. In Fig. 3, we show the direct ionization cross section with and without the contribution of ionization-excitation processes (solid and dashed lines, respectively) for the Pd-like ions of Sn^{4+}, Ba^{10+}, Nd^{14+}, Tb^{19+}, Yb^{24+}, and W^{28+}. Effects of ionization-excitation processes can easily be seen for all ions from barely ionized Sn^{4+} to highly ionized W^{28+}. Without the contribution of the ionization-excitation processes, the cross section will be underestimated by a few percent to 15% (for Gd^{18+}). Toward lower ionized ions from Gd^{18+}, the fraction of underestimation is stabilized to be the same value of about 12% for Nd^{14+}, Ba^{10+}, and Sn^{4+}. This value is nearly constant for all Pd-like ions from Sn^{4+} to Gd^{18+}, independent of specific ions. Toward the direction of increasing ionization stages from Gd^{18+}, the fraction of underestimation is 9%, 5%, and 5% for Tb^{19+}, Yb^{24+}, and W^{28+}, respectively. This value decreases from 15% for Gd^{18+} to 9% for Tb^{19+} and then stabilizes to 5% for a wide range of Pd-like ions. The dominant ionization-excitation channels are levels belonging to the configuration of $4s^24p^64d^84f$.

Ionization-excitation processes are, in general, much weaker than those of the pure direct ionization for light- and medium-Z elements. Bellm *et al.* [36,37] experimentally measured the differential ionization-excitation cross-section ratios for the $n = 2$–4 states of He$^+$ relative to the direct

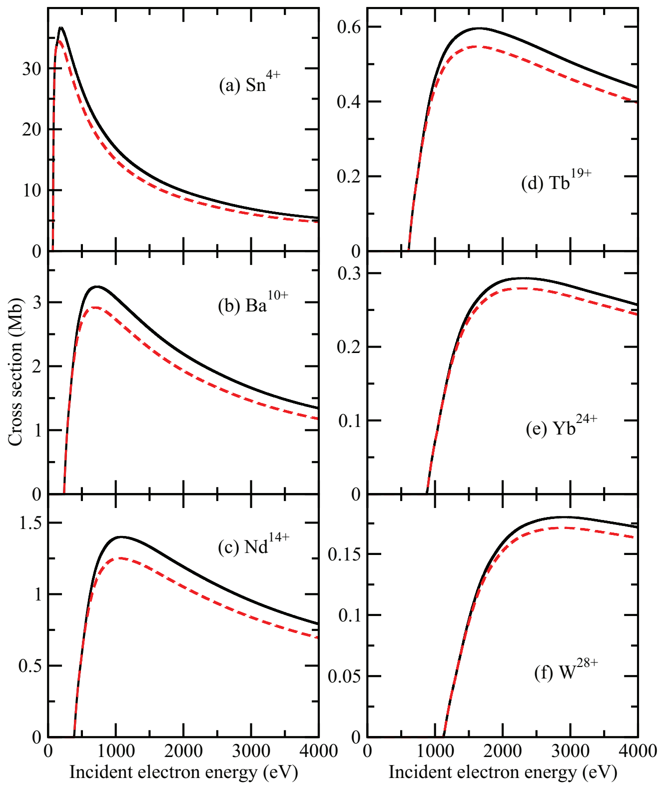

FIG. 3. (Color online) Ionization cross section with and without contributions from the ionization-excitation processes for Pd-like ions of Sn^{4+}, Ba^{10+}, Nd^{14+}, Tb^{19+}, Yb^{24+}, and W^{28+}.

ionization of He by electron impact, and their results confirmed this conclusion. They further demonstrated that second-order approximation is necessary in their hybrid distorted-wave and convergent R-matrix approach. Thus the use of the first Born approximation of Eq. (1) might lead to inaccuracy in the cross section. Including the higher-order effects might lead to more accurate results, but it does not affect our conclusion. However, the effects of ionization-excitation processes cannot be neglected for heavy ions. Why is this so? Such effects are entirely due to electron correlations. In Fig. 4 we show the square of radial wave functions of $4d$, $4f$, and $5f$ orbitals for Sn^{4+}, Gd^{18+}, and W^{28+}. They are obtained from a self-consistent Dirac-Fock-Slater iteration on a fictitious mean configuration with fractional occupation numbers, representing the average electron cloud of the configurations included above. To adequately describe the initial and final states of electron impact processes, we have included extensive electron correlations including single and double excitations from the respective ground configuration. The electron correlation is vital for obtaining an accurate EII cross section, and its effects have been demonstrated in research fields such as the radiative opacity of hot, dense, high-Z plasmas [38–40]. By inspecting Fig. 4, one can know the reason why the ionization-excitation processes have evident contributions to the total ionization cross section from the viewpoint of the radial wave function. For the barely charged ion of Sn^{4+} [Fig. 4(a)], there is a definite overlapping between the radial wave functions of $4d$ and nf ($n = 4,5$). This means that the transition matrix element of $\langle 4d|\frac{1}{r_{4d-4f}}|nf\rangle$ ($n = 4,5$) in Eq. (1) is large. With the increase

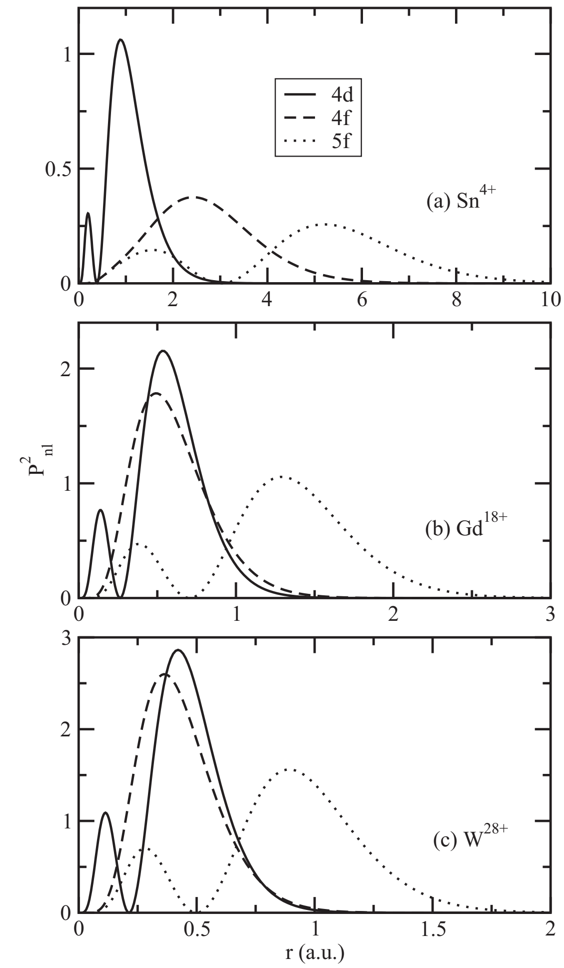

FIG. 4. Square of the radial wave functions of orbitals $4d$, $4f$, and $5f$ for (a) Sn^{4+}, (b) Gd^{18+} and (c) W^{28+}.

of the atomic number (Gd^{18+} and W^{28+}), the wave function of $4f$ tends to be inward compared with that of the $4d$ orbital. The $4f$ orbital shows collapse characteristics. From the radial wave functions of $4d$ and $4f$, we can understand the basic feature of ionization-excitation processes. In fact, this is a general phenomenon for heavy ions with outmost subshells of $4d$ and $5d$.

IV. CONCLUSION

The detailed level-to-level ionization cross section of the $4s^24p^64d^{10}$ ground level of Gd^{18+} is investigated theoretically by using a fine-structure-level distorted-wave approximation from the threshold to 4000 eV. The ionization-excitation cross section due to excitation of levels in the $4s^24p^64d^84f$ configuration is comparable to the direct ionization cross sections of $(4s^24p^54d^{10})_{1/2}$ and $(4s4p^64d^{10})_{1/2}$. If the contribution from these ionization-excitation channels is neglected, the total ionization cross section can be underestimated by a few percent to about 15%. For heavy atomic ions, this is a general phenomenon. We demonstrate this conclusion by investigating the ionization-excitation cross section of Pd-like ions of Sn^{4+}, Ba^{10+}, Nd^{14+}, Tb^{19+}, Yb^{24+}, and W^{28+}. For the barely charged ion Sn^{4+}, there is definite overlapping between the wave functions of the $4d$ and nf ($n = 4,5$) orbitals. With the increase of the atomic number, the $4f$ orbital moves inward and collapses, which results in a considerable overlap of $4d$ and $4f$ electrons.

ACKNOWLEDGMENTS

This work was supported by the National Natural Science Foundation of China under Grant Nos. 11274382 and 11274383.

[1] T. R. Kallman and P. Palmeri, Rev. Mod. Phys. **79**, 79 (2007).
[2] A. Müller, Adv. At. Mol. Opt. Phys. **55**, 293 (2008).
[3] J. Y. Dai, Y. Hou, and J. M. Yuan, Phys. Rev. Lett. **104**, 245001 (2010).
[4] M. Mattioli, G. Mazzitelli, M. Finkenthal, P. Mazzotta, K. B. Fournier, J. Kaastra and M. E. Puiatti, J. Phys. B **40**, 3569 (2007).
[5] K. Dere, Astron. Astrophys. **466**, 771 (2007).
[6] A. Borovik, Jr. *et al.*, J. Phys. B **46**, 175201 (2013).
[7] M. S. Pindzola *et al.*, J. Phys. B **46**, 215202 (2013).
[8] P. F. Liu, Y. P. Liu, J. L. Zeng, and J. M. Yuan, Phys. Rev. A **89**, 042704 (2014).
[9] J. L. Zeng, P. F. Liu, W. J. Xiang, and J. M. Yuan, Phys. Rev. A **87**, 033419 (2013).
[10] J. L. Zeng, P. F. Liu, W. J. Xiang, and J. M. Yuan, J. Phys. B **46**, 215002 (2013).
[11] W. J. Xiang, C. Gao, Y. S. Fu, J. L. Zeng, and J. M. Yuan, Phys. Rev. A **86**, 061401(R) (2012).
[12] U. Stamm, J Phys. D **37**, 3244 (2004).
[13] J. L. Zeng, C. Gao, and J. M. Yuan, Phys. Rev. E **82**, 026409 (2010).
[14] C. Wagner and N. Harned, Nat. Photonics **4**, 24 (2010).
[15] G. Tallents, E. Wagenaars, and G. Pert, Nat. Photonics **4**, 809 (2010).
[16] B. W. Li *et al.*, Appl. Phys. Lett. **102**, 041117 (2013).
[17] B. W. Li *et al.*, Appl. Phys. Lett. **101**, 013112 (2012).
[18] J. Rausch *et al.*, J. Phys. B **44**, 165202 (2011).
[19] D. H. Zhang and D. H. Kwon, J. Phys. B **47**, 075202 (2014).
[20] A. Moy, C. Merlet, X. LIovet, and O. Dugne, J. Phys. B **47**, 055202 (2014).
[21] D. L. Moores and K. J. Reed, Adv. At. Mol. Opt. Phys. **34**, 301 (1994).
[22] P. Burke, C. Nobel, and V. Burke, Adv. At. Mol. Opt. Phys. **54**, 237 (2007).
[23] D. C. Griffin and M. S. Pindzola, Adv. At. Mol. Opt. Phys. **54**, 203 (2007).
[24] K. Wang *et al.*, At. Data Nucl. Data Tables **98**, 779 (2012).
[25] K. Wang *et al.*, J. Phys. B **43**, 175202 (2010).
[26] T. M. Shen, C. Y. Chen, Y. S. Wang, Y. M. Zou, and M. F. Gu, Phys. Rev. A **76**, 022703 (2007).
[27] T. M. Shen, C. Y. Chen, Y. S. Wang, Y. M. Zou, and M. F. Gu, J. Phys. B **40**, 3075 (2007).
[28] F. Li, G. Y. Liang, M. A. Bari, and G. Zhao, Astron. Astrophys. **556**, A32 (2013).
[29] G. Y. Liang, N. R. Badnell, and G. Zhao, Astron. Astrophys. **547**, A87 (2012).
[30] J. L. Zeng, G. Zhao, and J. M. Yuan, At. Data Nucl. Data Tables **93**, 199 (2007).
[31] O. Zatsarinny and K. Bartschat, J. Phys. B **47**, 061001 (2014).
[32] O. Zatsarinny and K. Bartschat, Phys. Rev. Lett. **107**, 023203 (2011).
[33] M. F. Gu, Can. J. Phys. **86**, 675 (2008).
[34] A. Kramida, Y. Ralchenko, J. Reader *et al.*, Atomic Spectra Database, http://physics.nist.gov/asd3.
[35] G. C. Rodrigues, P. Indelicato, J. P. Santos, P. Patte, and F. Parente, At. Data Nucl. Data Tables **86**, 117 (2004).
[36] S. Bellm, J. Lower, and K. Bartschat, Phys. Rev. Lett. **96**, 223201 (2006).
[37] S. Bellm *et al.*, Phys. Rev. A **75**, 042704 (2007), and references therein.
[38] J. L. Zeng and J. M. Yuan, Phys. Rev. E **74**, 025401(R) (2006).
[39] J. L. Zeng and J. M. Yuan, Phys. Rev. E **76**, 026401 (2007).
[40] J. L. Zeng, J. Phys. B **41**, 125702 (2008).